Gebremariam *et al. Herit Sci (2016) 4:32*
DOI 10.1186/s40494-016-0101-6

Heritage Science

RESEARCH ARTICLE

Open Access

Multi-analytical investigation into painting materials and techniques: the wall paintings of Abuna Yemata Guh church

Kidane Fanta Gebremariam*, Lise Kvittingen and David Graham Nicholson

Abstract

Abuna Yemata Guh is one of the nine Saints who are traditionally claimed to have come to Northern Ethiopia in the beginning of the sixth century and established monasteries in the Tigray region. The church, named after him, is hewn out of the side of one of the highest sandstone spires in the Gheralta area. Though the local tradition claims earlier dates, the paintings in the church are suggested to belong to the second half of the fifteenth century on the basis of their theme, style and iconography. We report here the investigation into the materials and techniques of the paintings using diverse complementary analytical techniques: Polarized light microscopy (PLM), portable X-ray fluorescence spectrometer (pXRF), scanning electron microscopy-energy dispersive X-ray spectroscopy (SEM–EDS), synchrotron-based X-ray diffraction (SR-XRD), pyrolysis gas chromatography-mass spectrometry (Py-GC/MS), micro-Raman spectroscopy (MRS) and micro-Fourier transform infrared spectroscopy (micro-FTIR). Earth materials based on hematite, goethite and terra verte were the main findings, but cinnabar, orpiment, lead white and carbon black were also identified. The stratigraphic analyses of samples from different locations coupled with SR-XRD analysis indicated the presence of anhydrite, gypsum, calcite and lime in the preparation layer. The pigments identified together with close visual examination showed repainting and retouching within the area in which the Marian figure is depicted, as well as in a nearby figure. The ground preparatory layer consisted of red mud reinforced by straw applied to the chiseled sandstone support. The egg-based binding medium suggests that tempera technique was used. Technical studies of Ethiopian wall paintings are scant, but highly needed as this world heritage is threatened due to limited conservation. Our documentation of the materials and techniques is therefore aimed to stem this loss, as well as to provide information for art historical studies.

Keywords: Abuna Yemata Guh church, Wall painting, Ethiopian painting, Ethiopian art, Multi-analytical techniques, Pigments, Painting technique, SEM–EDS, SR-XRD, Raman spectroscopy

Background

Abuna Yemata Guh Church is one of the most spectacular cliff-top rock-hewn churches in Ethiopia. It is carved into the side of one of the tall sandstone spires in the rocky mountains of Gheralta, Tigray region (Fig. 1). The standing pillars are made up of Enticho and Adigrat Sandstones and considered as the last erosional remnants of a sandstone plateau that once covered the Precambrian basement [1]. According to local legend, the church was hewn in the sixth century and dedicated to Abuna Yemata, one of the Nine Saints. The Nine Saints are traditionally believed to have originated from Rome, Constantinople and Syria between the end of the fifth and beginning of the sixth centuries [2, 3]. They were engaged in the expansion of Christianity, establishment of a monastic tradition, translation of the Holy Christian scriptures into the ancient Ethiopian language, Geez, that is the language of the liturgy of the church still today. Radiocarbon dating of an illuminated manuscript, Abuna Garima Gospel, belonging to, and named after, another member of the Nine Saints is dated between fifth and sixth century [4], thus giving substance to the Christian

*Correspondence: fanta@ntnu.no
Department of Chemistry, Norwegian University of Science & Technology (NTNU), 7491 Trondheim, Norway

Fig. 1 **a** The site of Abuna Yemata church with its surroundings. The *arrow* shows the location of the church. **b** A close-up view of the entrance leading to the door (as indicated by the *arrow*)

art history at that time. The paintings in Abuna Yemata Guh church have been dated to fifteenth–sixteenth century based on thematic composition as well as stylistic and iconographic grounds [5].

Access to the church is one of the most difficult in the country. A strenuous ascent is followed by a climb up a vertical rock wall depending entirely on hand grips and foot holds (without additional support) crowned with a walk over a 50 cm wide ledge facing a cliff of 300 m sheer drop. However, entering the church is rewarding, as these paintings are magnificently striking to the extent that one can temporarily forget the awaiting return descent.

As opposed to many church wall paintings in Ethiopia, the paintings in Abuna Yemata Guh, are in a relatively well-preserved state. The lower parts on the walls, which have been exposed to human contact during services, and parts that have been covered by curtains are severely affected by loss of painting materials and detachments. The dry condition in the local environment, the painting technique and the columnar sandstone roofing could have contributed to the relatively good conservation state of the paintings and their survival. Almost all the walls, the cupolas and columns are covered by paintings portraying the Apostles, the Nine Saints, Abraham, Jacob, Isaac, Mary and Christ, Angles, Moses, Paul, Peter, saints, monks (like Abuna Kiros, Abuna Mattewos, Abba Esi), as well as interlacing decorations. Some of these figures are shown in Fig. 2. The design of the traceries in Abune Yemata Guh church replicates those found in nearby churches of Gheralta, such as Debre Tsion church. There are a greater number of paintings depicting figures from the Old Testament than from the New Testament.

Though some studies on the paintings from art historical perspective have been conducted [2], there are no previous technical investigations on the painting materials and techniques of the murals of the church. The aim of this investigation is to contribute to a better understanding of the materials and techniques employed in execution of the murals. Such documentation and analysis support both conservation-restoration interventions and art historical studies with relevances to dating, authentication, attribution, provenance of materials and production technology studies.

Methods

Following in situ examination with a portable X-ray fluorescence spectrometer (pXRF), samples were collected and analysed by optical microscopy (OM), scanning electron microscopy-energy dispersive X-ray spectroscopy (SEM–EDS), micro-Raman spectroscopy (MRS), micro-Fourier transform infrared spectroscopy (Micro-FTIR), synchrotron-based X-ray powder diffraction (SR-XRD) and pyrolysis gas chromatography-mass spectrometry (Py-GC/MS). Cross-sectioned samples were prepared in order to study the paint stratigraphy, the composition and morphology of the support, preparatory and painting materials.

Fig. 2 The paintings of Abuna Yemata Guh church depicting the Apostles on the cupolas, and Moses, Paul, Peter and Thomas among others on the wall and column. The *figures* are identified by descriptions in Geez calligraphic script that accompany them in accordance with the Ethiopian painting traditions

Sampling

In situ analyses using a pXRF (see instrumental techniques, under) were conducted for preliminary identification of pigments and to guide sample collection. Twenty-five pXRF measurements on green, yellow, red, white and black painted areas were taken. Multiple measurements on each type of colour from different sites were conducted to assess similarities in chemical composition. Micro samples from the scenes depicting Virgin Mary and Child, Abba Esi and Abuna Yemata Guh were extracted with a scalpel from areas already damaged and loosened. The sample colours were green, red, yellow, white, black and green.

Sample preparation

Samples, or grains detached from the samples, were used without preparation when necessary (for OM and MRS), or prepared according to the requirement of the analytical techniques to be used. Cross-sectioned samples were made by embedding the sample in a fast light-curing methacrylate based resin (Technovit® 2000 LC, Heraeus Kulzer) and used in OM, SEM–EDS, SR-XRD and MRS investigations. Diamond cell was used to prepare the required sufficiently thin samples for micro-FTIR measurements in transmission mode.

Instrumental techniques

Portable X-ray fluorescence spectrometry (pXRF)

The pXRF investigations were carried out in situ using a Niton XL3t 900 (Thermo Fisher Scientific) portable energy-dispersive XRF analyser, equipped with a miniaturized X-ray tube coupled to a high-performance, thermoelectrically cooled Si-PIN diode detector. A silver anode X-ray tube (50 kV, 40 μA, 2 W maximum) with a polyimide film (Kapton®) was used to access the energies of a wide range of elements including the light ones. The analyser is fitted with an internal CCD camera for closer visualization of the measured painting spot. Collimating the primary beam to 8 mm diameter, instead of 3 mm, was sufficient to cover the details on the wall paintings, at the same time maximizing the X-ray fluorescence detected. The instrument was run in the Cu/Zn mining mode. Additional descriptions of the instrument and the parameters selected are given elsewhere [6]. The concentrations of the elements were obtained by means of the algorithm for the fundamental parameters using the factory-set internal calibrations. The data, which were treated as semi-quantitative, were used just to estimate the relative proportions of the elements. Qualitative identification of the elements based on the spectral interpretation was mainly applied in this study.

Optical microscopy (OM)

The examinations of non-embedded samples and cross-section preparations were performed using an AmScope stereomicroscope, fitted with a 10MP digital camera and a Carl Zeiss Axio Imager polarized light microscope. In the latter case, an AxioCam MRc5 (Zeiss) camera and the Carl Zeiss AxioVision software were used for microphotography and graphics processing.

Scanning electron microscopy-energy dispersive X-ray spectroscopy (SEM–EDS)

A HITACHI S-3400 N scanning electron microscope equipped with an energy-dispersive spectrometer (Oxford AZtec Microanalysis System, with an 80 mm^2 X-MaxN Silicon Drift Detector) was used for the elemental analysis and mapping. The accelerating voltage was 15 kV and the working distance set at 10 mm. The cross-section samples were sputter-coated with carbon to avoid charging effects prior to SEM–EDS examination.

Synchrotron-based X-ray powder diffraction (SR-XRD)

The SR-XRD was performed on the Swiss-Norwegian Beam Line (SNBL)/(BM01A) at the European Synchrotron Radiation Facility (ESRF), Grenoble, France. A hybrid pixel detector PILATUS 2 M (Dectris) was used with the wavelength calibrated to 0.70065 Å, and a sample-to-detector distance of 444 mm. A series of measurements were taken at different spots on the cross-section samples. These covered sequentially the preparatory and painting layers.

The cross-section samples with thin thicknesses, a few millimeters after grinding and polishing with sand paper to reduce the size of the resin, were mounted between Kapton® support sheets. The diffraction patterns were processed using the program Fit2d [7], which integrates the Debye–Scherrer rings acquired from the 2D detector to the equivalent 2-theta scan. The Bruker DiffracPlus EVA software and the ICDD PDF4 database were used for processing the data and for identifying phases. The crystallographic and graphic program WinPLOTR (from the FullProf Suite [8]) was also used for processing the SR-XRD data.

Micro-Fourier transform infrared spectrometry (Micro-FTIR)

For the micro-FTIR measurement, a Perkin-Elmer Spotlight 200 infrared imaging microscope interfaced to a Spectrum One Fourier transform infrared spectrophotometer (Perkin Elmer) was used. The IR system uses a 100 × 100 mm liquid nitrogen-cooled mercury cadmium telluride (HgCdTe) detector. Samples for measurement were prepared by pressing small grains of the sampled material in a diamond anvil cell. The measurements were carried out in transmission mode using aperture sizes 50 × 50 and 100 × 100 micrometers. Following the application of pressure, the samples adhering to each diamond window were investigated. A clean part of the

diamond cell was used to collect the background spectrum. Each spectrum collected in the infrared range of 4000–550 cm^{-1} represents the average of 16 individual scans and has a 4 cm^{-1} spectral resolution. The software Spectrum and Image were used in the data collection and processing. The spectroscopy software Spekwin32 [9] was also used in processing the data.

Micro-Raman spectroscopy (MRS)

The Raman spectra were acquired using a Jobin–Yvon LabRAM HR800 confocal Raman spectrometer, fitted with a Peltier-cooled CCD detector. The parameter settings were as follows: a 600 grooves/mm holographic grating, a 200 μm slit width and a 785 nm diode laser source adjusted to 0.8 mW at the sample by an appropriate filter. The laser was focused on particles of the sample using objectives of 50× and 100× magnifications. The LabSpec software was used to display the spectrum and for the subsequent processing.

Pyrolysis gas chromatography-mass spectrometry (Py-GC/MS)

Samples (about 0.1 mg or less, placed in a quartz tube with quartz wool beneath and on top) were admixed with 8 μl of tetramethylammonium hydroxide (TMAH) solution (25 % in water, Sigma-Aldrich) and pyrolysed at 850 °C for 10 s. The CDS Pyroprobe 5250 (Chemical Data Systems) pyrolyser was coupled (online) to a 7890A gas chromatography system (Agilent Technologies) and a 5975C mass selective detector (Agilent Technologies). The GC parameters were: column, DB-5MS UI, 30 m × 0.25 mm × 0.250 μm, phenyl-arylene/methylpolysiloxane; split mode (1:50); injection port temperature 300 °C; carrier gas helium, flow rate; 1 mL/min; temperature program: start 60 °C (6 min hold), 20 °C/min to 340 °C (2 min hold). The MS parameters were as follows: transfer line temperature/heater 300 °C, electron impact ionization (EI) mode; ionization energy 70 eV. The GC–MS ChemStation software was used for data collection and the NIST 08 MS Library for identifying the pyrolysis products.

Results and discussions

Characterization of the painting technique

Structure of the painting

The general painting programme appears to be uniform, but there are indications of repainting and retouching at a later period (as will be discussed later). Optical examination of the stratigraphy in the cross-sections, SEM–EDS investigations, as well as preliminary Py-GC/MS analysis, suggest a secco painting technique where the pigments were applied with organic binder on a dried plaster. The stratigraphy of the paintings was generally made of four parts as shown in Fig. 3a; the sandstone support (actually the mountain wall), a mud-based layer, a preparatory layer and finally a painting layer. The sandstone support has been roughened (to increase adhesion) with indentations, as can be seen on walls not covered by paintings (Fig. 3b). The earth mud preparation containing straws was applied onto the sandstone to level the rough surface in order to accommodate the finer preparation layer of the plaster. The straw improves the tensile strength of the mud layer and reduces the tendency to crack. The mud layer serves as the arriccho in the context of buon or true fresco painting. Earth-based plaster strengthened with straw has been identified in ancient Egyptian painting [10], a post-Byzantine church in Greece [11], as well as a church in Ethiopia [12]. Straw reinforcement (based on the cereal teff, *Eragrostis abyssinica*, a crucial indigenous staple in Ethiopia) is a common structural element in mud houses in the country. Fibre reinforced mud structures are subjects of recent investigations that have shown the enhanced properties achieved due to the use of plant fibrous materials like the straw inclusions [13–18]. The fine-textured preparatory layer was applied thinly onto the earth/mud preparation and in turn made to receive the painting layer. In Europe, the chalk or gypsum based ground preparations for panel paintings common in the Middle Ages were replaced by clayey-earth ground preparations especially in the Baroque paintings (seventeenth–eighteenth centuries) [19, 20].

Characterization of painting materials

The nature of support, preparatory and painting layers used

The pXRF results are summarized in Table 1, with descriptions of the colours, the location of the measurement area, the elemental composition and the pigments identified. This information will be further discussed in light of results from complementary methods.

Support and preparatory layers

In the preparatory layer calcium was identified by pXRF. SR-XRD analyses of a yellow sample showed the presence of anhydrite ($CaSO_4$) as the major constituent and gypsum ($CaSO_4{\cdot}2H_2O$) and bassanite ($CaSO_4{\cdot}1/2H_2O$) as minor ones of both the preparatory and painting layers. Calcium appears to be highly correlated with strontium, a correlation also previously observed in other cultural heritage objects [21] and Ethiopian wall paintings [6]. This relation appears to be linked to the mineral source used to produce the gypsum ($CaSO_4{\cdot}2H_2O$) or the calcite ($CaCO_3$) and may in general provide a marker to distinguish between gypsum obtained from a mineral source

Table 1 Result of on-site pXRF analyses of the murals of Abuna Yemata Guh church

SN	Colour	Origin	Elements detected	Pigments implied
1	Yellow	Part of cloak of Aba Esi, right of St Mary's figure	**Fe, As, Ca, S, S**i, Mg, Cl, Sr	Orpiment, calcite and\or gypsum
2	Yellow	Getse kelb, from head part, under the figure of AYG	**Fe, Si, Ca,** S	Yellow ochre
3	Yellow	Part of cloak of Aba Esi, right of St Mary's figure (see also 1)	**As, S, Ca,** Fe, K	Orpiment and calcite and\or gypsum
4	Yellow	Geometric figure, interlace below the figure to the left of Abuna Yemata	**Fe,** Mn, Ca	Yellow ochre
5	Yellow	Part of a geometric interlacing figure below St Mary's figure, remnant from a damaged part	**Ca, Fe, Si,** S	Yellow ochre
6	Yellow	Part of the geometric figure (damaged) below a man figure to the left of Mary with Christ	**Fe, Ti,** Mn	Yellow ochre
7	Red	Part of throne, right side close to the lower border, Mary with Child figure (see also 13)	**Pb, Hg, S, Fe**	Red ochre, cinnabar, and lead white
8	Red	Center of the geometric figure, interlace described in 4	**Fe, Ca, S,** Zn., Mn, Ni, Co, K, Ti	Calcite based, some gypsum
9	Red	Part of throne, close to the lower border, right side, Mary with Child figure	**Fe, Ca, S**, **K**, Mn, Cu, Ni	Yellow ochre based
10	Red	Lower border, Mary with Child figure	**Hg, Fe,** As, Pb	Red ochre, cinnabar and lead white
11	Red	Part of throne, close to the lower border, left side, Mary with Child figure	**Hg, Fe**, As, Pb	Red ochre, cinnabar and lead white
12	Red	Lower border, Mary with Child figure	**Pb, Hg, Cu, Fe,** Ni, As	Red ochre, cinnabar and lead white
13	Red	Part of throne, right side close to the lower border, Mary with Child figure	**Pb, Hg, Cu, Fe, Ni, Ti**, S, Co, Mn, As,	Red ochre, cinnabar and lead white
14	Red	Part of throne, right side close to the lower border, Mary with Child figure (see also 13)	**Pb, Hg, S, Fe**	Red ochre, cinnabar, and lead white
15	White	Leftover in a damaged part below 22	**Fe, Ca, S,** Mn, Ni, Cu	Calcite and\or gypsum
16	White	Left over in a damaged part below 22 close to a yellowish damaged part	**Fe, Ca, S,** Mn, Cu, Ti	Calcite based, some gypsum
17	White	Part of a geometric decorative figure below St Mary's figure, remnant from a damaged part	Fe, Si, **Ca, Cl, S**	Calcite and\or gypsum
18	White	Part of the interlacing in the geometric figure described in 4 and 8	**Fe, Mn, Ca, S**, Zn, Ni, Cu. Ti	Red ochre
19	Olive Green	Part of (left side) cloak of Aba Esi, located to the right of St Mary's figure	**S**, Cl, **K**, **Ca, Si,** Ti, **Fe**	Green earth, calcite, gypsum
20	Green	Part of the geometric figure (damaged) below a man figure to the left of Mary with Christ	**Fe, Ca, S**	Green earth, calcite, gypsum
21	Green	Part of the interlacing in the geometric figure described in 4,8 and 18	Fe	Green earth
22	Red, earth support	Exposed part of the geometric figure (damaged) below a man figure to the left of Mary with Christ figure	**Fe, Ti**, Mn	Red ochre rich
23	Red, earth support	Exposed part of the geometric figure (damaged) below a man figure to the left of Mary with Christ figure	**As, Pb, Hg, Ca, Fe, S**, Co, Mn, K	Red ochre rich
24	Red, earth support	Exposed support made up of red earth, lower left cloth of St Mary, close to 11	Fe	Red earth

The major components identified are shown in boldface

and gypsum formed as an alteration product of calcite [21]. Here, however this relation was not further investigated. In a SEM–EDS analysis of a light reddish colour sample, that contains red ochre and gypsum, the presence of small grains of strontium sulphate was identified in both painting and preparatory layers, indicating most probably an association of the elements in the source material. Before the application of the thin white preparatory layer, a brownish straw-strengthened mud-based layer was applied (Fig. 3a).

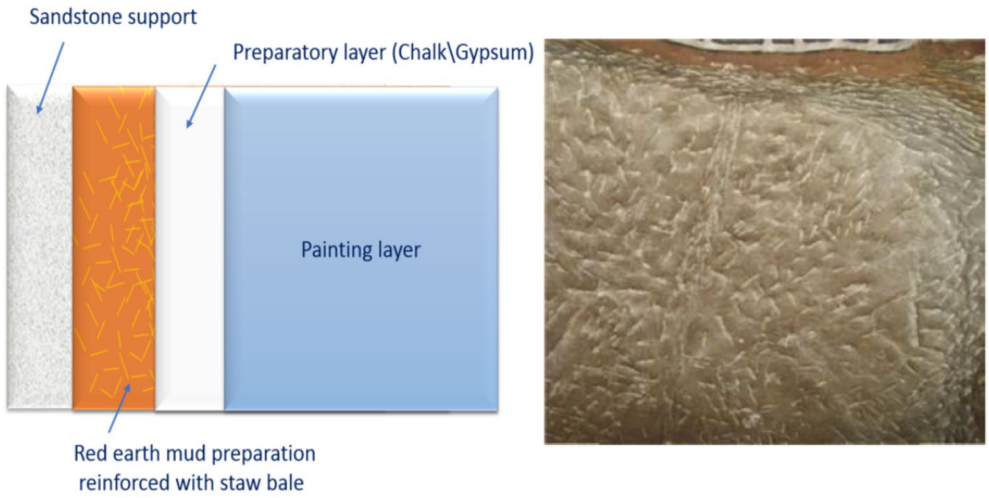

Fig. 3 **a** *Schematic diagram* showing the different layers of the wall painting structure. The pigments are applied on a gesso preparation that was prepared over a mud reinforced with straw. This red earth based preparation made the attachment to the sand stone support possible. **b** Part of the sand stone with the chisel marks not covered with paintings. Small fraction of the painted portion is visible in the *top part*

Painting layer

Yellow in the major painting programme The in situ examination (pXRF) indicated the use of two different pigments for the yellow colourant. The main yellow pigment throughout the paintings is likely to be yellow ochre as elevated concentrations of iron and silicon were associated with the ochre matrix. Aluminum belonging to the aluminosilicates is difficult to detect by pXRF (Table 1), but, SEM–EDS analysis of grains showed aluminum as well as silicon in high concentrations corroborating the possible use of yellow ochre. SR-XRD analyses revealed, as mentioned above, the calcium sulphate minerals anhydrite ($CaSO_4$), gypsum ($CaSO_4{\cdot}2H_2O$) and bassanite ($2CaSO_4{\cdot}H_2O$) with the former being the major component. The colouring pigment is goethite (FeO(OH)).

Yellow in the Marian figure The simultaneous detection of arsenic and sulphur in the pXRF examination of the bright yellow colour, typical of orpiment, in the Marian figure, and some near-by figures points to the use of orpiment. Visual examination of the yellow colour used on Mary's figure, painted on the western surface of one of the two columns separating the second and third bay and on some near-by figures, does not resemble yellow earth (Additional file 1). This bright yellow colour is more typical of orpiment than realgar (yellowish orange) and parareal-gar (red orange) that are also composed of arsenic and sulphur. The simultaneous detection by pXRF of arsenic and sulphur are consistent with orpiment. Therefore, it is likely that these figures are later repaints and retouches. See Fig. 13 for enhanced images of orpiment painted portions in contrast with other yellow colourants used. Orpiment was clearly identified based on the pXRF spectrum from a yellow painted area as well as Raman spectrum and elemental mapping in SEM–EDS obtained from a cross-section sample (Table 1; Fig. 4; Additional file 2). The Raman spectrum was compared with a reference library [22].

The lustrous golden tone of the orpiment was used to colour the cloth and nimbus of Jesus and the decorative motives including the cross on the cloth of Mary. It appears to have been used here as an imitation of gold. Orpiment was called 'The Kings's Gold' for its brilliance and resemblance to gold. The use of orpiment as a pigment extends over a very long period of time that could reach as far back as the seven century BC in Mesopotamia, where its source was also identified [10]. It was widely used in Asia for long period and in the Middle Ages orpiment was exported to Europe from Asia Minor [23]. Though it is possible that this pigment was originally from the Middle East, it could also have been obtained from the Dallol Depression (also called Danakil Depression) in Afar, northeast Ethiopia. Here, where volcanic and hydrothermal activities occur, the formation of sulphur and sulphide minerals are possible including sulphides of arsenic [24]. The search for the source of the orpiment used in this painting would thus benefit from further investigation.

Red

Red in the major painting programme The painting layer is a composite consisting of a matrix of clay-like cement into which the silica grains and red ochre pigment are incorporated. The SEM–EDS and the complementary

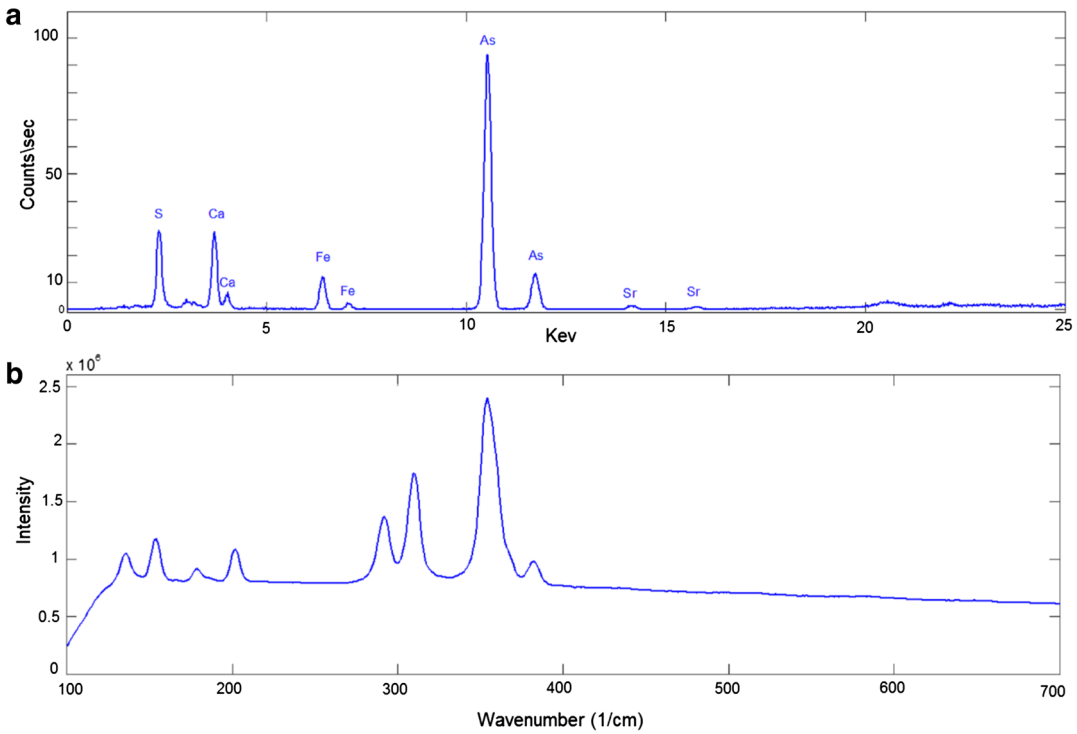

Fig. 4 **a** XRF spectrum obtained during the in situ examination of the yellow pigment used in the Marian Fig. **b** The corresponding Raman spectrum from the painting layer

pXRF in situ analyses data show that the red colour is due to iron (see the red colours in Table 1). SR-XRD analysis on a cross-section of the red sample enabled to identify the constituent minerals as being quartz, gypsum, hematite, calcite, lime and clay (some of the SEM–EDS results are given in the Additional file 3). FTIR spectra collected from a red sample have also shown similarity to a sandy red rock material collected in the vicinity of the church (Fig. 5). Pure ferric oxide is expected to show two strong bands: one in the range 557–577 cm^{-1} and the other around 475 cm^{-1} [25, 26]. In the sample it is indicated by the band centered at about 544 cm^{-1}, and the second one at a lower frequency is not visible (as the spectra were collected between 4000 and 500 cm^{-1}). Similar bands at 545 and 555 cm^{-1} were observed for the caput mortuum and hematite reference materials, respectively [27]. The clay

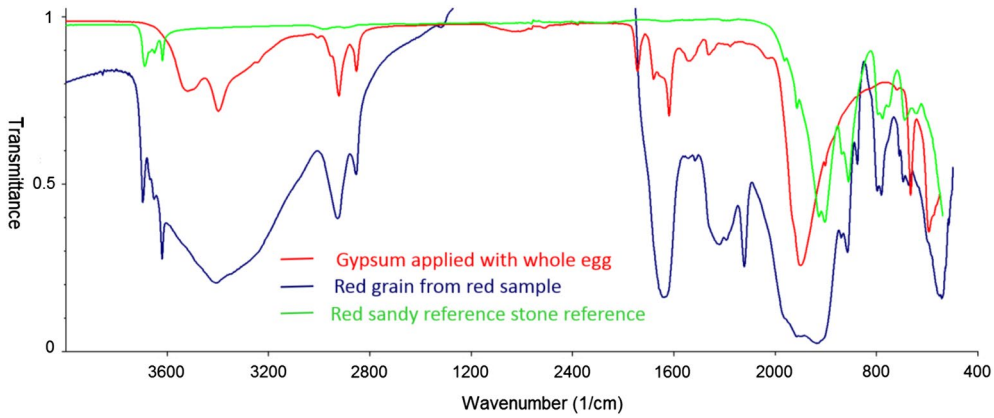

Fig. 5 Micro-FTIR spectrum taken from a red sample compared to spectra of reference materials: gypsum applied with whole egg (yolk and glair) and a sandy red rock sample collected from locality of the church

and silica components are indicated by their respective bands as can be compared with the reference spectra and absorption band assignments (Fig. 5). The quartz main peak appears at 1082 cm^{-1} (Si–O stretching) [26–28]. The Si–O–Si intertetrahedral bridging bonds in quartz (six- and eight-membered rings) can be easily recognized by the characteristic doublet at 780–798 cm^{-1} [28, 29]. An interesting feature is associated with the vibrations of the oxygen atom in bridging Si–O–Si groups expected at 1122 cm^{-1}. Both in the sample and reference spectra, it is shifted to 1118 cm—indicating high temperature heat treatment of the silica in the red ochre [30].

The clay components are indicated by the Si–O–Si strong broad band centered at 1041 cm^{-1}, along with the Si–O–Al band expected at 1011 cm^{-1}. The bands at 941 and 914 cm^{-1} represent the Al–O–H vibrations [26–28]. Other clay linked features include bands observed at 3696, 3668, 3654 and 3622 cm^{-1} that are assigned to the outer hydroxyl ions in the structures of the clay components [26, 28]. The presence of kaolinite both in the sample and reference materials can be recognized by the doublets at 914 and 941 cm^{-1} [28]. The broad band centered around 3408 cm^{-1} is due to the presence of moisture and includes parts of the bands from gypsum water of crystallization.

The earth pigments that are based on a clay matrix are the most stable pigments that have been in continuous use as painting materials since pre-historic times. In earth pigments, the main chromophore responsible for imparting the colour can be a non-clay component like the oxides of iron (hematite, goethite, magnetite) or chromogenous elements (like Fe^{2+} or Fe^{3+}) in the structure of the clay components, as is the case with green earth materials (glauconite, celadonite, smectites and chlorites) [20, 31]. When found together, both earth pigments change tint of each other's colour.

Red in the Marian figure In the church's Marian figure, an intense scarlet colour was used for parts of Mary's cloth, the throne, decorating the nimbus of Jesus, and in the frame surrounding the figure. It is distinct from the red earth based pigment used in the larger composition of the church painting. The main red pigment used was identified as cinnabar. The identification is based on the complementary results of in situ pXRF analysis, SR-XRD, SEM–EDS and Raman investigations on a micro sample (Table 1; Fig. 6). The presence of lead white transformation products like cerussite and platernite are also detected (Fig. 6). A closer examination of the painting stratigraphy using SEM–EDS showed lead white underpainting with earth-based layer beneath it as shown in Fig. 14 and described in later section. Some of the grains of cinnabar, mostly in fine grain sizes, and the distribution of the lead (associated with the lead-based pigment and its deterioration products), are indicated in the elemental mapping (Fig. 14e).

Grey green\olive green

The pXRF result indicated the use of green earth by the presence of potassium, iron and silicon. The lighter elements constituting green earth, aluminum and magnesium, are difficult to detect under the experimental setup used in the field (that is without helium purge). However, later surface examination of a grey green grain under vacuum condition in SEM–EDS analysis clearly showed most of the constituent elements of green earth like celadonite, $K(Mg,Fe^{2+})(Fe^{3+},Al)[Si_4O_{10}](OH)_2$, or glauconite, $(K,Na)(Mg,Fe^{2+},Fe^{3+})(Fe^{3+},Al)(Si,Al)_4O_{10}(OH)_2$, as shown in Fig. 7. The elements of the ground preparations such as anhydrite are also part of the spectrum as indicated by calcium and sulphur.

Gypsum, calcite and green earth were also identified in a grey green sample using micro-FTIR. Figure 9 shows the spectrum of a grain of a grey green sample displayed along with the reference spectra. The two well-resolved stretching modes near 3494 and 3404 cm^{-1} are due to the water of hydration in gypsum. The corresponding bending mode appeared at 1618 cm^{-1} [32, 33]. The spectrum of the sample shows calcium carbonate due to the presence of a strong band centered around 1428 cm^{-1}, characteristics of the C–O stretching mode of carbonate along with narrow bands around 876 and 715 cm^{-1} [34]. Part of the strong band centered around 1128 cm^{-1} and the small peaks at 674 and 602 cm^{-1} are assigned to the stretching and bending modes of sulphate, respectively. Close matching between the bands of the sample and most of the bands of a green earth reference is observed.

Dark grey green

The composition of the dark green sample was found to be similar to that of the grey–green sample. SEM–EDS showed the components of the green earth as well as grains of gypsum/anhydrite on the surface (Fig. 7; Additional file 4). In the SR-XRD investigations, the concentration of anhydrite was found to be high together with minor concentrations of lime and gypsum. The anhydrite in the dark grey–green painting layer may stem from the preparatory layer, where it is a major constituent (Fig. 10; Additional file 4). In addition, micro-FTIR and SR-XRD showed the possible use of celadonite-based green earth (Fig. 9; Additional file 4). As there are closely related clay based green earth minerals, like celadonite and glauconite, unequivocal identification using solely elemental techniques is precluded. Along with the typical appearance of the green earth painting layer (as shown in Fig. 8) the results of multiple techniques (pXRF, SEM–EDS,

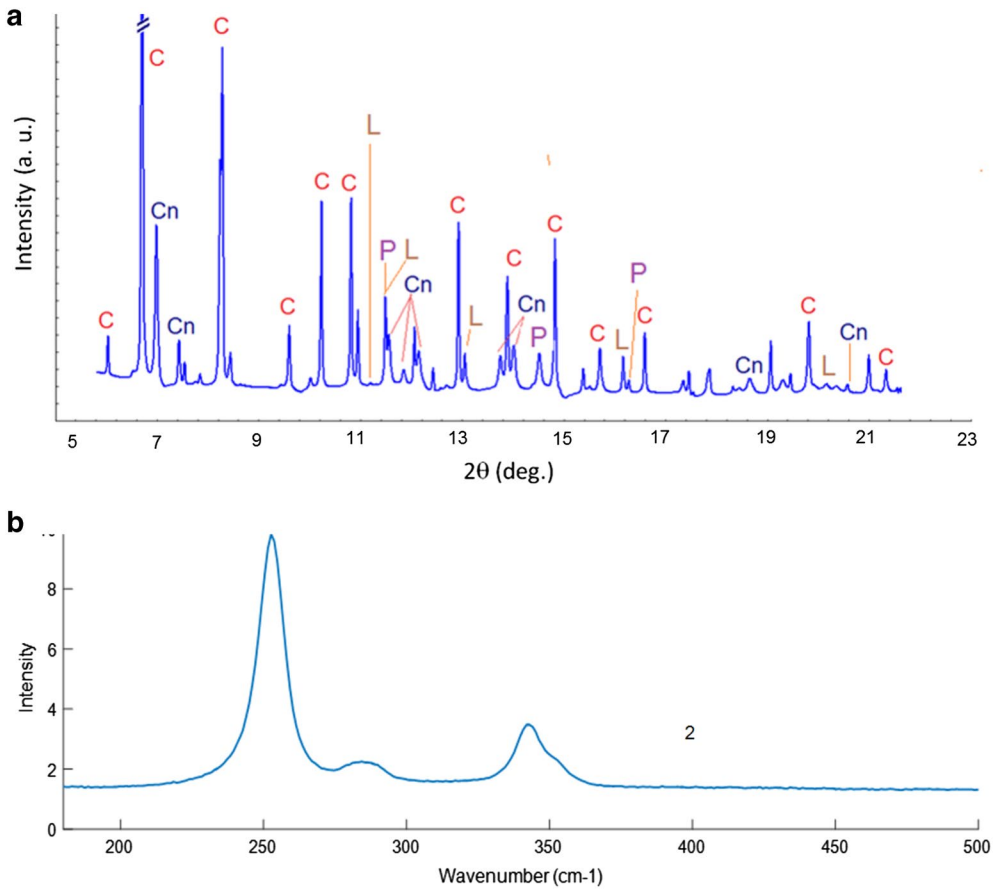

Fig. 6 **a** The SR-XRD pattern of a red sample used in the Marian figure showing the main inorganic components of the ground preparation and painting layer in the repaint (C-calcite, Cn-cinnabar, P-platernite and L-lead carbonate (cerussite) and **b** Raman spectrum obtained from a grain in the red painting layer confirming the presence of cinnabar

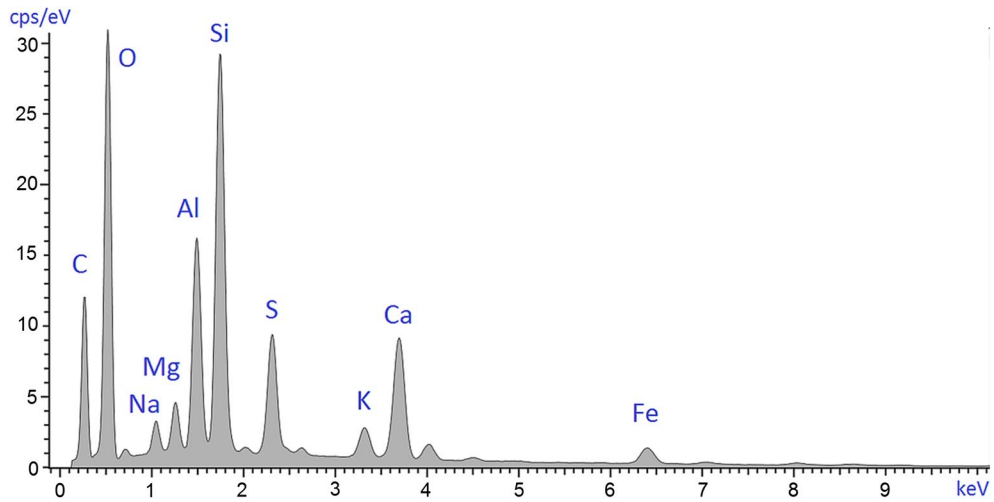

Fig. 7 SEM–EDS spectrum from a surface of a green sample (taken as a line average spectrum) thereby inferring the possible existence of gypsum\anhydrite, calcite and components of green earth. The spectrum is consistent with the composition indicated by the results from the green areas with pXRF. Grains of calcite and gypsum/anhydrite and calcite were similarly identified. A SR-XRD analysis of a green sample in cross-sections has shown the use of calcite and anhydrite as the preparatory layer components (Fig. 10)

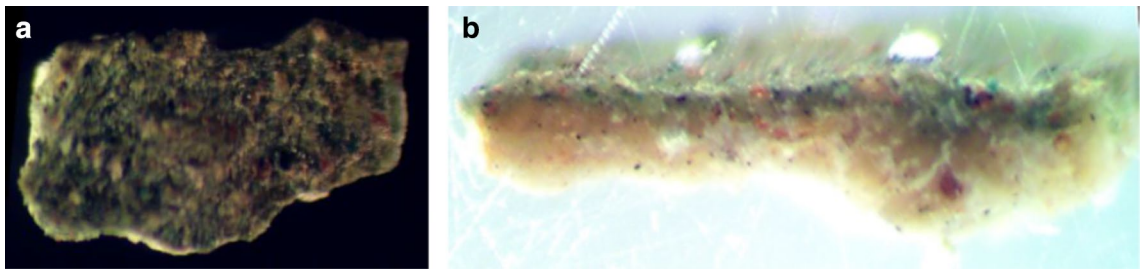

Fig. 8 Green sample **a** top view and **b** the corresponding cross-section. The combination of pXRF, SEM–EDS, and SR-XRD reveals that the *colour* stems from green earth

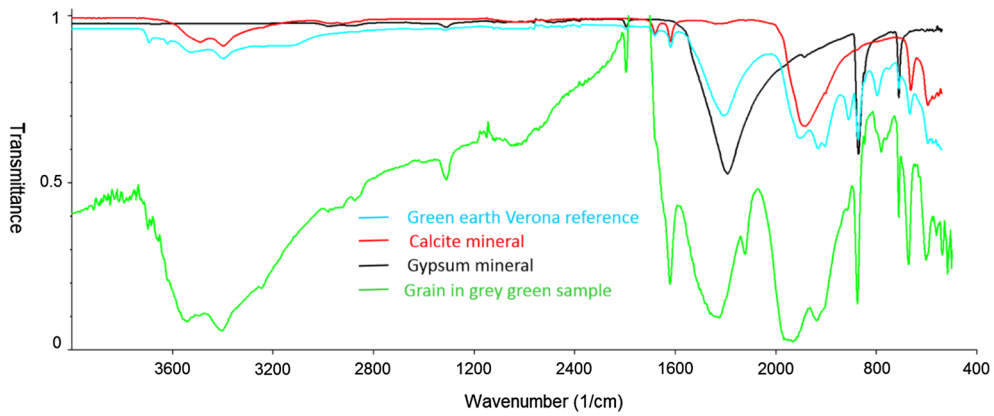

Fig. 9 IR spectra of a grey green sample along with reference spectra indicating the presence of green earth, gypsum and calcite

micro-FTIR and SR-XRD) support green earth being the pigment employed in the green tone colourations (Table 1, Figs. 7, 8, 9; Additional file 4).

White

The white pigment was characterized by pXRF (Table 1) and SEM–EDS (Fig. 11) as being calcite. The former technique also revealed the presence of sulphur along with calcium, which could be consistent with calcite undergoing possible conversion to gypsum or anhydrite. The presence of aluminosilicates, iron and other transition metal elements such as manganese and titanium are attributed to dust that has accumulated on the surface and possibly to partly exposed areas of the earth-based preparation layer.

Black

The pXRF of a black painted area showed the presence of calcium, iron and potassium. Figure 12 shows the front and back surfaces of a sample of black paint with the latter revealing a red-based layer that is reinforced by straw. Calcium is associated with the preparatory layer but the iron content could originate from the deposition of dust onto the surface. The SEM–EDS indicates a high concentration of carbon in the paint layer from which we infer that carbon black or soot black is the pigment. Other types of black pigment (e.g. bone black, ivory black, and manganese oxide) contain manganese and/or phosphorus which were not detected thereby ruling out the possible use of these pigments. In addition to the morphological examination of the cross-section preparation and SEM–EDS analysis, FTIR spectroscopy supported the conclusion drawn as spectra of bone black, ivory black and carbon black were compared with one obtained from the black sample.

Pigments suggesting a possible repainting

From the composition of the pigments, it appears that the image portraying Mary and the Child does not accord with the overall painting programme because the palette used here includes cinnabar, orpiment and lead white, which is different from the earth pigments used elsewhere for the same colours, namely red and yellow ochres. These differences in types of pigment suggest that the Marian figure may have been painted after the rest of

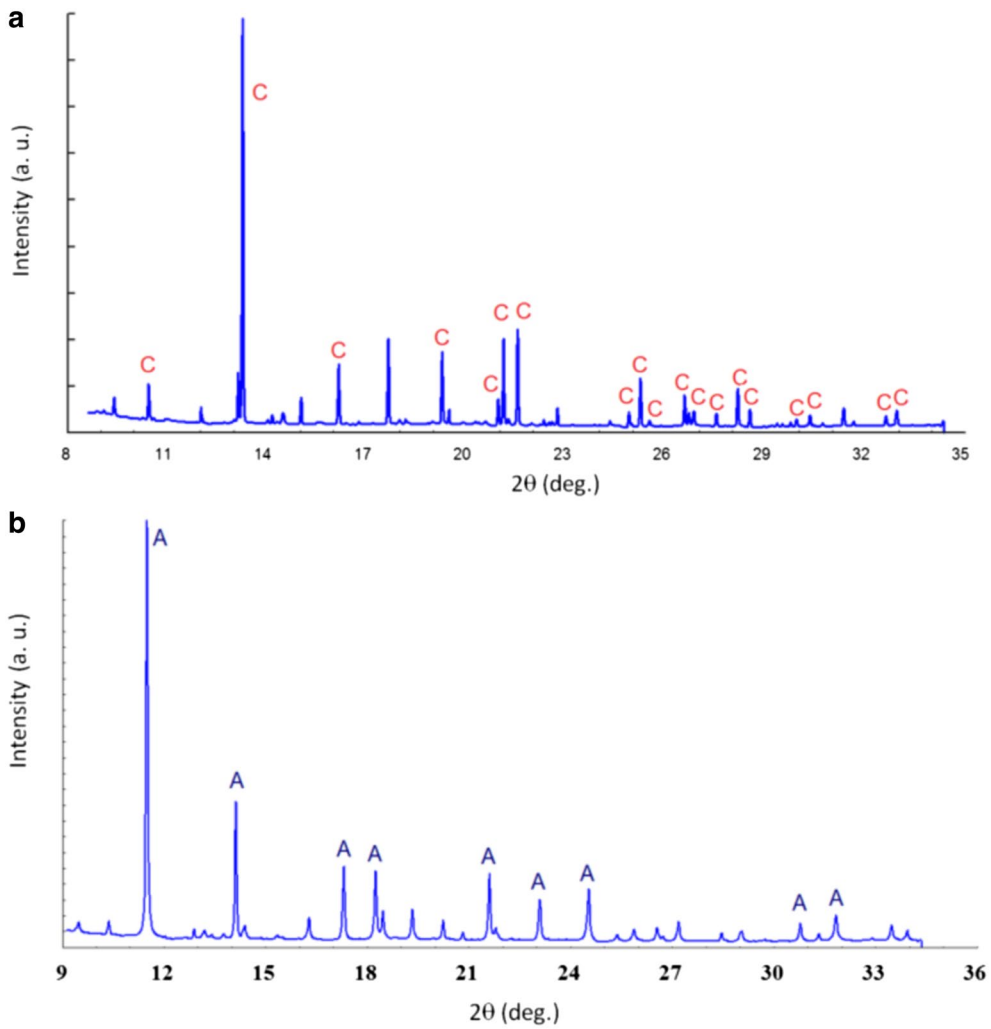

Fig. 10 SR-XRD pattern of green sample indicating **a** the calcite, **b** the anhydrite in different layers of the same cross-sectioned sample

the murals (together with some retouches in the neighbouring figure).

This is substantiated by the cross-section analysis (Fig. 14) which revealed an earlier painting layer in the Marian figure similar to the green painting layer observed in the major painting programme. Taken together, these results suggest that this part of the painting stems from a later period, though the Marian figure follows the style of the older paintings, including the accompanying Geez inscription. It is apparent from close visual examination that there is overlapping between this part of the mural and the rest (Fig. 13). We therefore suggest that the dating of the paintings in the church may need to be revisited if this is primarily based on the Marian figure. Supporting information may be forthcoming from the composition of the other paintings, in which narratives from the Old Testament are predominant, and comparing the paleography of the inscriptions with older Geez scripts.

The SEM–EDS examinations also support the Marian painting being a later addition as traces of earlier layer, probably coloured green using terra verte, are indicated. From the BSE image and elemental mapping it is apparent that the older and newer painting layers are separated at their interface that could lead to detachment (Fig. 14c, d).

Organic binding medium investigation

The organic binder used in the green and white samples was investigated using Py-GC/MS. The Py-GC/MS analysis (Additional file 5) revealed fatty acids, and dicarboxylic acids in a sample taken from a white painted area,

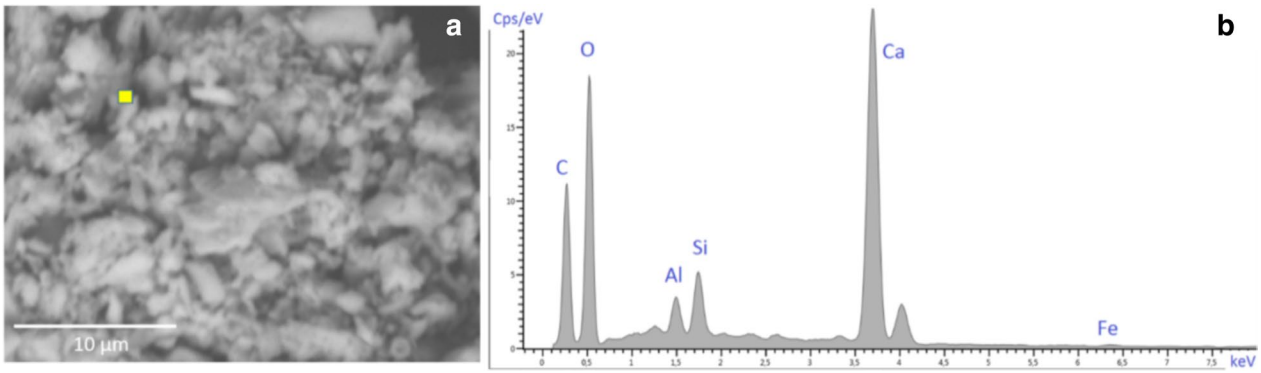

Fig. 11 SEM–EDS analysis of the surface of a grain of white sample. **a** BSE with the analysis spot (shown in *yellow*) and **b** a spectrum from spot analysis showing the use of calcite for the white colouration. Components of clay (aluminosilicates) particles are also indicated in the spectrum

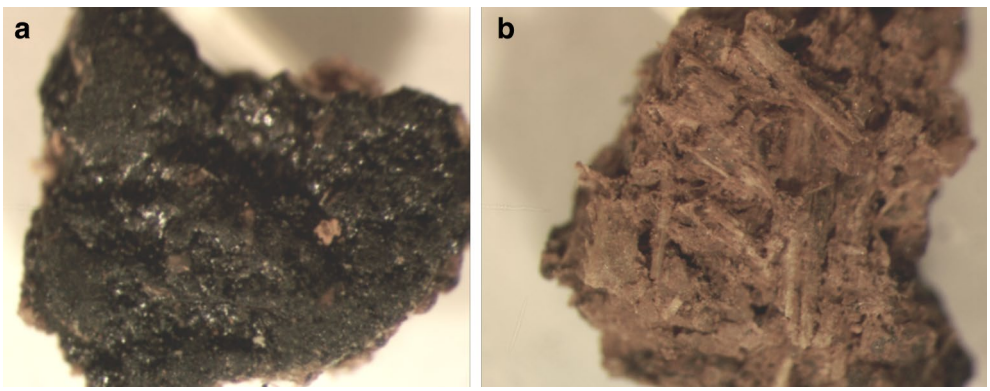

Fig. 12 Black sample front appearance (**a**) and back (**b**) indicating the mud-based layer applied with straw to enhance strength and attachment to the sandstone support

which indicates the use of a drying oil such as linseed oil. In comparison with a reference sample chromatogram, the use of egg is inferred applied possibly along with the drying oil. The dicarboxylic acids indicated can also originate from the use of egg but an intentional addition of siccative oil cannot be excluded. Pyrolysis products of protein-based binders were not identified thereby ruling out the use of animal glue. The phthalic and benzoic acids detected (Additional file 5) could have originated from the pyrolysis of lignin in plant materials, such as the straw used in the layer after the support. The methane sulphonic acid is derived from the anhydrite/gypsum in the preparatory layer. An identical chromatogram was obtained from a green paint sample used for the binder identification. The possible use of egg as a binder was also supported by the micro-FTIR investigation on a green paint sample.

Conclusions

Based on complementary methods, comprehensive information about materials and techniques in the murals of Abuna Yemata Guh church has been obtained. In almost all the samples examined, only a single painting layer was observed with the exception of the Marian painting, where an underlying painting layer was identified. The pigments are mostly based on minerals—earth pigments that can be acquired locally. Cinnabar and orpiment were identified in the Marian image and not elsewhere. Together with evidence from close visual examinations, possible repainting in that specific location is likely. The latter pigments, can have been of local origin, or might have been imported, depending on the period of the painting. Further investigation on the provenance is needed. There is also chronological implication based on the pigment identification as cinnabar and orpiment have

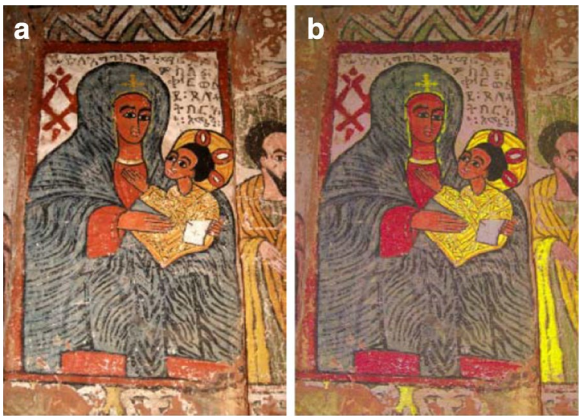

Fig. 13 The image of Mary and Child **a** without and **b** with colour enhancement using false colour. The retouched *bright yellow portion* is better contrasted through the use of the false colour compared to its appearance in the original (**a**)

been painted on top of the older paintings that are based on red ochre, yellow ochre and green earth.

Probably due to the dry microclimate in the church, the paintings are in a relatively good state except the lower walls parts that are accessible to human contact. Loss of the preparatory layer was observed in such exposed areas leading to the loss of the painting layer altogether. Conservation intervention to consolidate the loosened painting layer is needed. The identification of egg and drying oil in Py-GC/MS investigations and the stratigraphic analysis of the painting layers inferred the use of the secco painting technique on a dried plaster. Red earth mud with straw was used below the preparatory layer for the purpose of promoting strong adhesion to the support and leveling effect. The documentation of the painting materials and techniques of the wall paintings can support future conservation interventions and art historical studies.

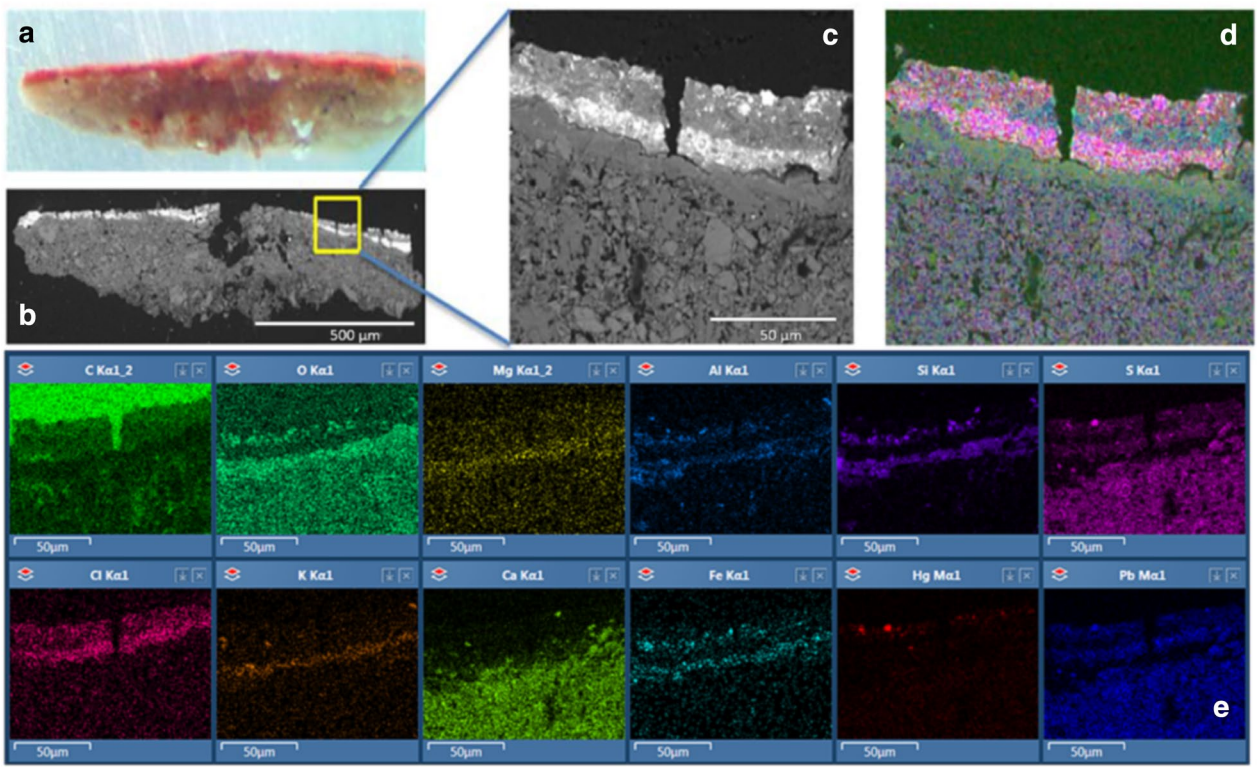

Fig. 14 Red sample from the Marian figure: **a** cross section under light microscopy in reflective mode, **b** the corresponding BSE image, **c** close-up image of the section highlighted in the *yellow box* in **b** showing the application of multi-painting layers and **d** the overlayered elemental mapping showing the ground preparation, older aluminosilicate based earth pigment applied, lead white layer, another earth based layer and finally the cinnabar layer that also contains calcite and lead white, **e** elemental mapping in the *yellow box* area selected. Spectral interference in the case of sulphur and lead is visible. The lead distribution is confined to the *top layer* as witnessed by the BSE image where lead appears bright along with mercury

Additional files

Additional file 1. Yellow retouched area: close-up image.

Additional file 2. Yellow paint sample investigation related.

Additional file 3. Red paint sample investigation related.

Additional file 4. Green paint sample investigation related.

Additional file 5. Binding media investigation related.

Authors' contributions

KFG carried out the fieldwork, prepared the samples, conducted the analysis and drafted the manuscript in consultation with LK. LK and DGN worked on the draft and revised it critically. LK facilitated the diverse investigations and follow-ups. DGN participated during the SR-XRD investigations. All authors read and approved the final manuscript.

Acknowledgements

The authors acknowledge the Ethiopian Orthodox Tewahedo church (EOTC) and the Ethiopian Authority for Research and Conservation of Cultural Heritage (ARCCH) for the facilitation during the field work, the Department of Chemistry, Faculty of Science and Technology, NTNU, and the NUFU program, financed by Norad, for financial support during the field work and analyses. Phil Pattison, Hermann Emerich and Wouter van Beek are appreciated for their support during the experimental period in the Swiss-Norwegian Beamlines (SNBL) of the European Synchrotron Radiation Facility (ESRF), JOTUN Group, for running samples in the Py-GC\MS analysis as well as Richard Verley for the linguistic input.

Competing interests

The authors declare that they have no competing interests.

Received: 2 March 2016 Accepted: 10 August 2016
Published online: 28 September 2016

References

1. Williams FM. Understanding Ethiopia: geology and scenery. New York: Springer; 2016.
2. Hable Selassie S. Ancient and medieval Ethiopian history to 1270. Addis Ababa: United Printers; 1972.
3. Votrin V. The orthodoxy and sustainable development a potential for broader involvement of the orthodox churches in Ethiopia and Russia. Environ Dev Sustain. 2005;7:9–21.
4. Bausi A. The "True Story" of the Abba Gärima Gospels. COMSt Newsletter; 2011. p. 17–20.
5. Lepage C, Mercier J. The ancient churches of Tigrai. Paris: ADPF; 2005.
6. Gebremariam KF, Kvittingen L, Banica F-G. Application of a portable XRF analyzer to investigate the medieval wall paintings of Yemrehanna Krestos church, Ethiopia. X-Ray Spectrom. 2013;42:462–9. doi:10.1002/xrs.2504.
7. Hammersley A. The FIT2D Home Page. 2016. http://www.esrf.eu/computing/scientific/FIT2D/. Accessed 20 Feb 2016.
8. FullProf Suite—a set of crystallographic programs. 2016. https://www.ill.eu/sites/fullprof/. Accessed 24 Feb 2016.
9. Menges F. Spekwin32—Optical Spectroscopy Software. Version 1.72.0. 2015. http://www.effemm2.de/spekwin/. Accessed 10 Dec 2015.
10. Rickerby S. Original painting techniques and materials used in the Tomb of Nefertari. In: Miguel AC, Mahasti A, editors. Art and eternity: the Nefertari Wall Paintings Conservation Project, 1986-1992. Marina del Rey: The Getty Conservation Institute; 1993. p. 43–53.
11. Daniilia S, Minopoulou E, Andrikopoulos KS, Tsakalof A, Bairachtari K. From Byzantine to post-Byzantine art: the painting technique of St Stephen's wall paintings at Meteora, Greece. J Archaeol Sci. 2008;35:2474–85. doi:10.1016/j.jas.2008.03.017.
12. Gebremariam KF, Kvittingen L, Banica FG. Physico-chemical characterization of pigments and binders of Murals in a church in Ethiopia. Archaeometry. 2015;58:271–83. doi:10.1111/arcm.12163.
13. Binici H, Aksogan O, Shah T. Investigation of fibre reinforced mud brick as a building material. Constr Build Mater. 2005;19:313–8. doi:10.1016/j.conbuildmat.2004.07.013.
14. Yetgin Ş, Çavdar Ö, Çavda A. The effects of the fiber contents on the mechanic properties of the adobes. Constr Build Mater. 2008;22:222–7. doi:10.1016/j.conbuildmat.2006.08.022.
15. Miccoli L, Müller U, Fontana P. Mechanical behaviour of earthen materials: a comparison between earth block masonry, rammed earth and cob. Constr Build Mater. 2014;61:327–39. doi:10.1016/j.conbuildmat.2014.03.009.
16. Bouhicha M, Aouissi F, Kenai S. Performance of composite soil reinforced with barley straw. Cement Concr Compos. 2005;27:617–21. doi:10.1016/j.cemconcomp.2004.09.013.
17. Danso H, Martinson DB, Ali M, Williams JB. Physical, mechanical and durability properties of soil building blocks reinforced with natural fibres. Constr Build Mater. 2015;101:797–809. doi:10.1016/j.conbuildmat.2015.10.069.
18. Quagliarini E, Lenci S. The influence of natural stabilizers and natural fibres on the mechanical properties of ancient Roman adobe bricks. J Cult Herit. 2010;11:309–14. doi:10.1016/j.culher.2009.11.012.
19. Grygar T, Hradilová J, Hradil D, Bezdička P, Bakardjieva S. Analysis of earthy pigments in grounds of Baroque paintings. Anal Biochem. 2003;375:1154–60. doi:10.1007/s00216-002-1708-x.
20. Hradil D, Grygar T, Hradilová J, Bezdička P. Clay and iron oxide pigments in the history of painting. Appl Clay Sci. 2003;22:223–36. doi:10.1016/S0169-1317(03)00076-0.
21. Franceschi E, Locardi F. Strontium, a new marker of the origin of gypsum in cultural heritage? J Cult Herit. 2014;15:522–7. doi:10.1016/j.culher.2013.10.010.
22. Burgio L, Clark RJH. S Library of FT-Raman spectra of pigments, minerals, pigment media and varnishes, and supplement to existing library of Raman spectra of pigments with visible excitation. Spectrochim Acta A Mol Biomol Spectrosc. 2001;57:1491–521. doi:10.1016/S1386-1425(00)00495-9.
23. Schafer EH. Orpiment and realgar in Chinese technology and tradition. JAOS. 1955;75:73–89.
24. Moussa N, Fouquet Y, Gall B, Caminiti AM, Rolet J, Bohn M, Etoubleau J, Delacourt C, Jalludin M. First evidence of epithermal gold occurrences in the SE Afar Rift, Republic of Djibouti. Mineral Deposita. 2012;47:563–76. doi:10.1007/s00126-011-0397-9.
25. Jacyna-Onyszkiewicz I, Grunwald-Wyspianska M, Kaczmarek W. IR studies of the phase transformation of $Fe_2O_3 \rightarrow Fe_3O_4$ by magnetomechanical activation. J Phys IV. 1997;07:C1-615–C611-616. doi:10.1051/jp4:19971255.
26. von Aderkas EL, Barsan MM, Gilson DFR. Application of photoacoustic infrared spectroscopy in the forensic analysis of artists' inorganic pigments. Spectrochim Acta A Mol Biomol Spectrosc. 2010;77:954–9. doi:10.1016/j.saa.2010.08.027.
27. Bikiaris D, Daniilia S, Sotiropoulou S, Katsimbiri O, Pavlidou E, Moutsatsou AP, Chryssoulakis Y. Ochre-differentiation through micro-Raman and micro-FTIR spectroscopies: application on wall paintings at Meteora and Mount Athos, Greece. Spectrochim Acta A Mol Biomol Spectrosc. 2000;56:3–18.
28. Bertaux J, Frohlich F, Ildefonse P. Multicomponent analysis of FTIR spectra: quantification of amorphous and crystallized mineral phases in synthetic and natural sediments. JSRC. 1998;68:440–7. doi:10.2110/jsr.68.440.
29. Sitarz M, Handke M, Mozgawa W. Identification of silicooxygen rings in SiO_2 based on IR spectra. Spectrochim Acta A Mol Biomol Spectrosc. 2000;56:1819–23.
30. Mamalimov RI, Shcherbako AI, Chmel AE. IR Spectroscopy study of the surface of commercial quartz ceramic specimens. J Appl Spectrosc. 2013;80:308–10. doi:10.1007/s10812-013-9764-x.
31. Konta J. Clay raw materials in the service of man. Appl Clay Sci. 1995;10:275–335.
32. Aines RD, Rossman GR. Water in minerals? A peak in the infrared. J Geophys Res. 1984;89:4059–71. doi:10.1029/JB089iB06p04059.
33. Seidl V, Knop O, Falk M. Infrared studies of water in crystalline hydrates: gypsum, $CaSO_4 \cdot 2H_2O$. Can J Chem. 1969;47:1361–8. doi:10.1139/v69-223.
34. Böke H, Akkurt S, Özdemir S, Göktürk EH, Caner Saltik EN. Quantification of $CaCO_3$–$CaSO_3 \cdot 0.5H_2O$–$CaSO_4 \cdot 2H_2O$ mixtures by FTIR analysis and its ANN model. Mater Lett. 2004;58:723–6. doi:10.1016/j.matlet.2003.07.008.